Magnetic-Field Driven By-Stable Switching of Magnetic Cantilevers/ Beams via Microscale Magnetic Controls

CNF Project Number: 2866-20
Principal Investigator(s): Amal El-Ghazaly
User(s): Ludovico Cestarollo, Karthik Srinivasan, Zexi Liang, Melody Xuan Lim

Affiliation(s): Electrical and Computer Engineering, Materials Science and Engineering; Cornell University

Primary Source(s) of Research Funding: National Science Foundation

Contact: ase63@cornell.edu, lc942@cornell.edu, ks934@cornell.edu, zl467@cornell.edu, mxl3@cornell.edu
Website(s): https://vesl.ece.cornell.edu

Primary CNF Tools Used: Heidelberg Mask Writer - DWL2000, SÜSS MicroTec Gamma Cluster Tool, ASML PAS 5500/300C DUV Wafer Stepper, Oxford 81 Etcher, Xactix XeF_2 Isotropic Silicon etch system, C&D SmartProP9000, DISCO Dicing Saw, Zeiss Ultra SEM, AFM - Veeco Icon, P7 Profilometer

Abstract:

The primary objective of this research is to establish large-deformation tactile displays using magnetic elastomer actuators. Magnetic actuators require reproducible, small-scale approaches for controlling the magnetic field gradient and direction used to drive the actuation. Over the past year our research group has been investigating the design and fabrication of micro-magnetic controls capable of generating localized magnetic fields and gradients necessary to actuate deformations in these magnetic elastomers. We have fabricated and optimized control micromagnets with different magnetic states and properties. The efforts have then been focused on experimentally demonstrating the ability of these control magnets to cause actuation via a system composed of a magnetic cantilever/beam.

Summary of Research:

One of the favored modes of actuation in large-scale mechanical systems (motors, relays, etc.) is magnetic because of its ability to generate large forces from relatively compact form-factors. However, the scaling down of magnetic actuation controls has posed numerous challenges. In the case of magnetic materials used for control, thin-film processing and smaller dimensions cause reduced flux density and demagnetization of the films. In the case of electromagnetic coils, the smaller size increases resistance and leads to unreasonably high-power consumption and heating. On the other hand, if successfully scaled down and integrated with Oersted-field or spintronic switching, magnetic actuation can potentially offer a low-power and compact solution to micro-actuators, including MEMS relays, microfluidic pumps, and novel haptic interfaces with the desired micrometer-scale resolution of magnetic fields and gradients [1-4].

This research project focuses on enabling the development of high-resolution, programmable haptic interfaces by developing a system of control magnets able to control the deflection of microscale beams/cantilevers.

A system of control magnets is designed to generate the local magnetic fields that would cause actuation. Two control magnets are engineered to have magnetizations preferentially pointing along two orthogonal axes, leading to the coupling of the magnetic flux densities between them and the generation of a field (and gradient) localized with micrometer resolution. These two control magnets are referred to as PMA (perpendicular magnetic anisotropy) and IMA (in-plane magnetic anisotropy) magnets. To investigate the ability of this system of magnets to generate useful forces for haptic applications, the team has designed a system composed of the two controls and an ALD (atomic layer deposition) beam/cantilever, which is made magnetic by embedding very thin soft magnets on its surface. The proposed design allows localization of a strong magnetic flux density and its gradient to a confined region of space between the two control magnets, enabling the magnetic actuation of the beam/cantilever with micro-scale resolution (Figure 1).

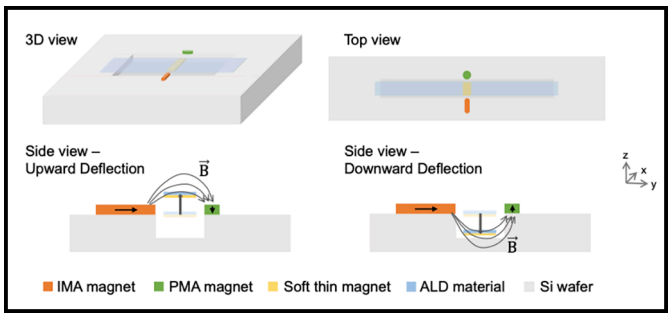

Figure 1: Magnetic actuation of a magnetic ALD beam via system of control PMA/IMA magnets.

Simulations have been designed and run to show that at these small microscales the generated magnetic flux density gradients between the two magnets are on the order of 10^4 T/m at vertical distances of hundreds of nanometers above (below) the magnets. These field gradients would act of the beam/cantilever by deflecting it to where the magnetic field is the strongest. This is at roughly 100 nm above the control magnets in the case of the PMA magnet being downward magnetized, and 100 nm below the magnets when the PMA magnet is upward magnetized.

The magnetic pull force exerted on the cantilever/beam, expressed as $F_z = m_x B_{xz} + m_y B_{yz}$ (where m=magnetic moment, and B=magnetic flux density), is computed. Simulations show that the B_{xz} component of the field gradient (rate of change of B_x as a function of z) is order of magnitudes larger than B_{yz}. This indicates that the soft thin magnets on the cantilever/beam should be designed with an elongated shape in the x-direction to promote magnetic anisotropy along this axis and maximize the magnetic force F_z. Furthermore, this magnetic force is shown to be greater than the mechanical force from the beam/cantilever, proving that the control magnets exert a magnetic field and gradient that are sufficient to mechanically deflect the beam/cantilever (Figure 2).

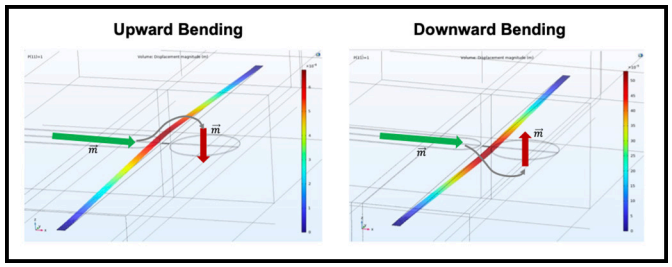

Figure 2: Magneto-mechanical simulation showing bipolar switching of a magnetic ALD beam via system of control PMA/IMA magnets.

The team is currently working on fabricating the system presented above. Deposition and patterning steps have been optimized to obtain the designed structures.

Conclusions and Future Steps:

This research shows that IMA and PMA magnets can be engineered and combined to generate magnetic flux density coupling useful for high-resolution magnetic actuation. Localization of a magnetic field (and a gradient) is achieved in a very narrow region of space with micrometer resolution. This system of magnets is integrated into a device with a narrow cantilever/beam, which is made responsive to applied magnetic fields by adding small magnets to it. In conclusion, this work will enable the realization of high-resolution, micrometer-scale magnetic actuators for haptics and numerous other mechanical applications.

References:

[1] L. Cestarollo, S. Smolenski, and A. El-Ghazaly, "Nanoparticle-based magnetorheological elastomers with enhanced mechanical deflection for haptic displays," ACS Applied Materials & Interfaces, vol. 14, no. 16, pp. 19002-19011, 2022.

[2] S. Marchi, et al., "Highly magneto-responsive elastomeric films created by a two-step fabrication process", ACS Applied Materials & Interfaces, vol. 7, no. 34, pp. 19112.19118, 2015.

[3] K. J. Dorsey, et al., "Atomic layer deposition for membranes, metamate-rials, and mechanisms," Advanced Materials, vol. 31, no. 29, 1901944, 2019.

[4] J. Streque, et al., "New magnetic microactuator design based on PDMS elastomer and MEMS technologies for tactile display," IEEE Trans. Hap-tics, vol. 3, no. 2, pp. 88-97, 2010.

Fabrication of Micro Scale Triboelectric Microphone

CNF Project Number: 2929-21
Principal Investigator(s): Shahrzad Towfighian
User(s): Mohammad Alzgool

Affiliation(s): Mechanical Engineering, Binghamton University

Primary Source(s) of Research Funding: National Science Foundation Grant #1919608

Contact: stowfigh@binghamton.edu, malzgoo1@binghamton.edu, mmalzgool14@gmail.com

Primary CNF Tools Used: YES Asher, Unaxis PT770, OEM AlN sputtering, AJA sputter deposition, Heidelberg DWL-2000 Mask writer, Oxford PECVD, Oxford 81 etcher, PT770 etcher, DISCO dicing saw, SÜSS MA6-BA6 contact aligner, YES polyimide curing oven, PRIMAXX vapor etcher

Abstract:

We were previously able to fabricate the smallest triboelectric generator and we used it for switching a MEMS parallel-plate switch and as an accelerometer. The generator was utilized as a vibration sensor by connecting it to a MEMS-switch, this switch operates once the frequency or acceleration of vibration surpasses a threshold, the operating modes are called frequency sensitive mode and acceleration sensitive mode. Nowadays, we are trying to fabricate a microphone that operates by using the mechanical structure and the triboelectric property of polyimide and aluminum with a back-etched wafer with aluminum nitride-aluminum layer as our diaphragm. The back-plate consists of polyimide and aluminum. The polyimide is thick and is a substitute for the amorphous silicon that we used in previous design as a proof mass. The motivation of this project comes from the promising results acquired from the MEMS triboelectric accelerometer which gave high signal-to-noise ration and the high and linear response of the output voltage.

Research Summary:

There are many advantages of triboelectric generators over piezoelectric generators such as lower cost, high flexibility, and superior electrical output. The operation of triboelectric generators depends on contact of a metal and a dielectric material with different affinity to electrons, the contact will result in charged conductive plates and separation with high impedance in between the plates will result in high voltage.

The triboelectric generator fabricated in this project was connected to a MEMS switch with a summer electronic circuit to apply DC voltage to the system (Figure 1). The triboelectric generator in this work is responsible for the AC voltage supply which is generated as a response to outside vibration excitation. When the vibration exceeds certain amplitude or frequency the switch closes as a result of the dynamic behavior of the MEMS switch which is characterized in previous works.

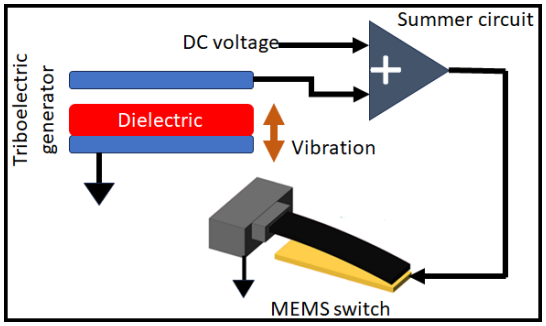

Figure 1: Experimental setup schematic.

Fabrication:

The fabrication process for triboelectric generator starts with aluminum nitride insulation, aluminum is sputtered and patterned for bottom electrode, polyimide spin-coating, curing, and patterning is carried out. This will result in the bottom layer of the generator. Then, the gap is created by silicon oxide layer which is patterned to create top layer anchors. And top layer is created by sputtering aluminum and depositing amorphous silicon for proof-mass.

Nowadays, we are trying to change the fabrication process so that polyimide layer is part of the top electrode and to have a hole under the bottom electrode to create a microphone. A triboelectric microphone as we envision will have a back-etched silicon wafer as sound inlet, a membrane of aluminum nitride which vibrates with input, a small gap between the membrane and the back-plate, and a back-plate of polyimide-aluminum pair. The design of membrane and the back-plate is carried out with frequency mismatching in mind to guarantee contact between them as sound is received.

The fabrication process starts with 500 nm deposition of aluminum nitride followed by 100 nm sputtering of titanium nitride-aluminum to create the diaphragm. Both layers are patterned using ICP-RIE PT770 etcher. Then, 1.0 μm sacrificial layer for the gap is deposited using PECVD and etched using oxford 81 RIE. Then, the inlets are made by back-etching the wafer which is done by depositing 100 nm aluminum nitride which is patterned with back-side-alignment. The aluminum nitride is used as a hard-mask for back etching which is done using Unaxis PT770 for > 1000 loops. For the top layer, we start with spin-coating and curing of polyimide (HDmicron PI 2574). Then, aluminum is sputtered on top and patterned with PT770. Patterned aluminum can be used as a hard mask for polyimide patterning which is done by RIE machine oxford 81 with CF_4-O_2 recipe. Finally, the wafer is diced and wire-bonded for testing.

Results:

The pull-in for the beam used in this work happens at 2.1 V statically. Dynamically, the generator provides AC voltage up to 0.6 V peak to peak. In frequency sensitive mode of operation, the pull-in happens at different frequencies depending on the applied DC voltage, at 1.6 V it happens at 10.6 kHz, and at 1.7 V it happens at 8.9 kHz as shown in Figures 2 and 3.

For amplitude sensitive mode, the acceleration was raised gradually in 10 seconds period while measuring the response of the beam, it was noticed that there is an amplitude of oscillation that provides AC voltage that is enough to close the switch. This experiment is shown in Figure 4.

Conclusions and Future Steps:

The triboelectric generator previously fabricated was useful for vibration measurements, it can operate a switch in different modes by using the dynamic of the switch and the generator. The output of the generator increases with the excitation amplitude and, thus, can drive the switch to close in amplitude sensitive mode once a threshold is past. And because the switch has natural frequency that changes with DC voltage, the frequency of the vibration that causes the switch to close can be tuned.

Currently, we are working on fabricating a triboelectric microphone by adding a back-etch to the fabrication process and swapping the position of the polyimide from bottom to top so that it will act as a dielectric and a proof-mass layer.

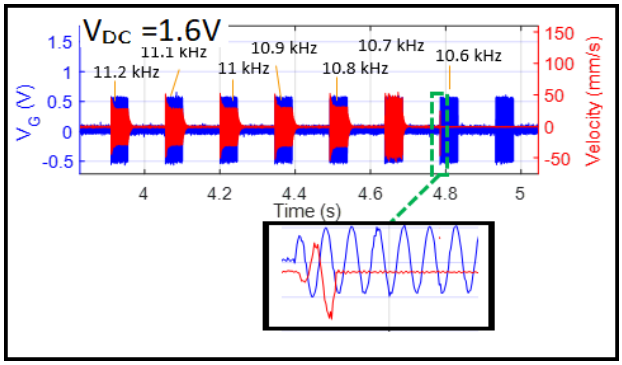

Figure 2: Frequency sensitive vibration sensor at V_{DC} = 1.6 V.

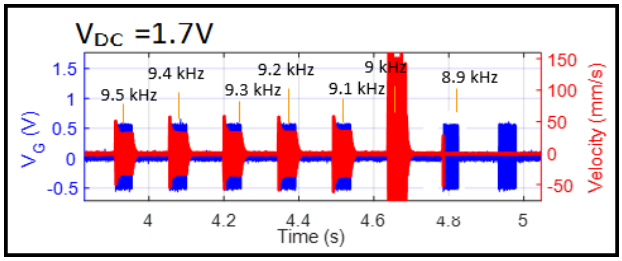

Figure 3: Frequency sensitive vibration sensor at V_{DC} = 1.7 V.

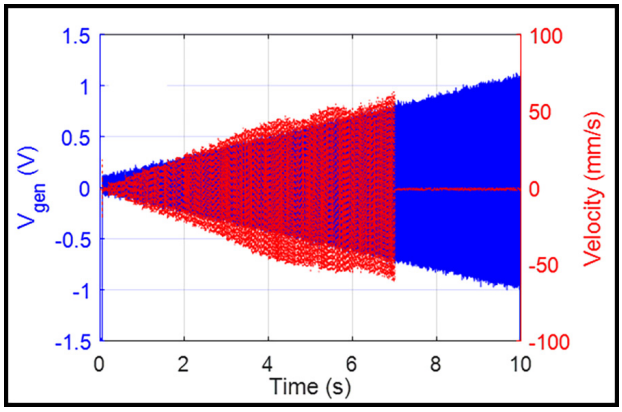

Figure 4: Acceleration sensitive vibration sensor.

References:

[1] Alzgool, M., Tian, Y., Davaji, B., and Towfighian, S. (2023). Self-powered triboelectric MEMS accelerometer. Nano Energy, 109, 108282.

[2] Mousavi, M., Alzgool, M., Davaji, B., and Towfighian, S. (2023). Event-driven MEMS vibration sensor: Integration of triboelectric nanogenerator and low-frequency switch. Mechanical Systems and Signal Processing, 187, 109921.

Programmable Microscopic Magnetic Self-Assembly

CNF Project Number: 2964-21
Principal Investigator(s): Itai Cohen, Paul L. McEuen
User(s): Zexi Liang, Melody Xuan Lim, Conrad Smart

Affiliation(s): Kavli Institute at Cornell for Nanoscale Science, School of Applied and Engineering Physics, Laboratory of Atomic and Solid-State Physics, Department of Physics; Cornell University

Primary Source(s) of Research Funding: National Science Foundation, Alfred P. Sloan Foundation

Contact: itai.cohen@cornell.edu, plm23@cornell.edu, zl467@cornell.edu, mxl3@cornell.edu, cs2239@cornell.edu

Primary CNF Tools Used: Oxford 81/82 etcher, YES EcoClean Asher, ASML DUV stepper, Gamma Automatic Coat-Develop Tool, JEOL 6300 EBL, SC 4500 odd-hour evaporator, AJA Sputter Deposition, Heidelberg DWL2000, PT770 etcher (left side), Unaxis 770 Deep Silicon Etcher, Plasma-Therm Takachi HDP-CVD, Oxford PECVD, Oxford ALD, Zeiss SEM, Veeco AFM

Abstract:

We develop an experimental platform for programmable microscopic magnetic self-assembly. We manufacture these microparticles at the wafer-scale, and have precisely designed shapes, magnetic moments, and magnetic interactions. Once released, we drive particles to explore their configuration space by a rotating magnetic field, generating chaotic flows that mix particles and drive assembly at the air-water interface. As a first example, we control self-limiting assembly by designing the shape and net magnetic moment of clusters at various stages in the assembly process. In particular, we show that spontaneous decoupling of the final product from the reaction forms a powerful principle for self-limiting assembly.

Summary of Research:

Recent progress has been made towards the self-assembly of structures that terminate at a finite size, rather than growing indefinitely. Such structures require a mechanism to detect when a cluster of a specific size is formed, and to prevent larger clusters from growing. Current strategies for such a self-sensing mechanism include geometric self-closing [1], geometric frustration [2], and strain accumulation [3].

Here, we demonstrate a new mechanism for non-equilibrium self-limiting assembly, which relies on programmable magnetic interactions between constituent particles. Our strategy makes use of the fact that the net moment of a magnetically assembled cluster is the vector sum of the constituent moments. We design a cluster which, when assembled, has no net magnetic moment and thus spontaneously decouples from external magnetic driving. This spontaneous decoupling ensures that once a cluster is fully formed, it achieves stability and ceases to interact with the external driving field.

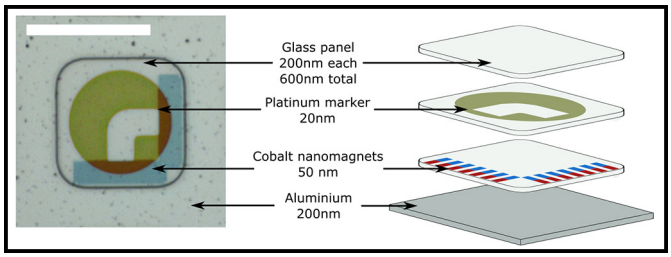

Figure 1: Schematic and optical microscope image of magnetic device layer structure.

Consequently, this halts the cluster's growth at a specific size, while other magnetically driven particles remain actively engaged in mixing and assembly.

Our devices are completely fabricated at CNF (see Figure 1 for device schematic). On top of a aluminum/aluminum oxide sacrificial layer, we pattern single-domain cobalt nanomagnets using electron-beam lithography [4] and metallize by liftoff. These nanomagnets are then embedded in silicon oxide thin films, whose shape and size are precisely patterned by a deep-ultraviolet (DUV) stepper. The combination of photolithography and electro-beam lithography allow us to pattern magnetic devices where the strength and shape of the magnetic interaction, placement of magnets, and contact interactions from the silicon oxide panel can all be harnessed to design a landscape for magnetic self-assembly.

We release these panels and observe their dynamics in the lab under an optical microscope. In order to do so, we deep reactive ion etch through the back of the silicon wafer, leaving only the sacrificial layers and magnetic devices. The magnetic devices are coated with a hydrophobic polymer layer, such that when TMAH solution is added to etch the sacrificial layer, the magnetic devices are released to float on the liquid-air interface.

Surface tension (combined with the hydrophobic particle surface) confines the particles to a single layer, allowing us to record and observe their interactions.

The very low friction environment of the liquid-air interface enables us to visualize the effect of small magnetic forces, as well as to introduce out-of-equilibrium driving. In this case, we use rotating magnetic fields to generate particle rotation. As the particles align to follow the applied magnetic torque, the fluid around them is forced to rotate with each particle. When particles are sufficiently close, these rotating hydrodynamic flows become collectively chaotic, acting to effectively mix particles and "thermalize" the system.

The exact parameters of the magnetic driving control the final distribution of assembly products (see Figure 2 for assembly design, and Figure 3 for distribution of final product as a function of magnetic driving). For example, if particles are consistently driven at a high amplitude (40 Oe) magnetic field, particles remain separated and do not assemble, since the magnetic torque dominates over local interactions that drive assembly. Driving particles at a small amplitude (10 Oe) magnetic field results in disordered aggregation: all products of the assembly are formed in equal proportion, since the magnetic driving is insufficient to thoroughly mix the particles. However, driving magnetic assembly at an intermediate magnetic field (20-30 Oe) produces the maximum conversion into the final assembly product. At this magnetic field condition, particles are able to overcome the applied torque and assemble into higher order products, while also being mixed sufficiently to explore their local environment.

We can further enhance the fraction of successfully assembled final product by dynamically changing the magnetic field driving conditions. This strategy makes use of the fact that the final assembled product spontaneously decouples from the external field, so that raising the magnetic driving to a high amplitude will break incomplete or undesired structures, but not the final product. As a result, cyclically lowering and raising the magnetic field will gradually enhance the number of particles that successfully assemble into the final product (see Figure 4).

This work demonstrates a general design principle for out-of-equilibrium self-limiting assembly by spontaneous decoupling. Future work will leverage these ideas to generate complex structures, particularly those that harness energy from external magnetic fields to perform useful work. Combining these principles with programmable magnetic bindings [4-6] will provide a powerful platform for complex, functional magnetic microstructures.

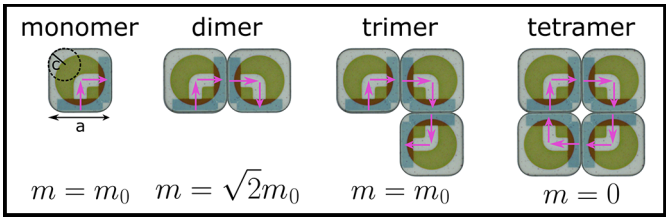

Figure 2: Schematic of assembly products from four identical magnetic devices, with magnetic moments indicated as arrows.

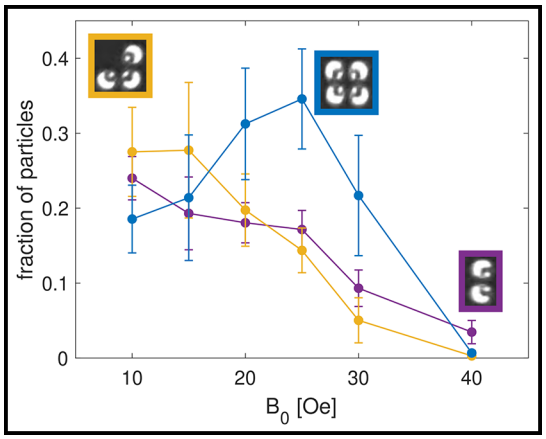

Figure 3: Plot of the distribution of assembly products (dimer, trimer, and tetramer) as a function of the amplitude of magnetic driving. The total yield (including monomer) sums to 1.

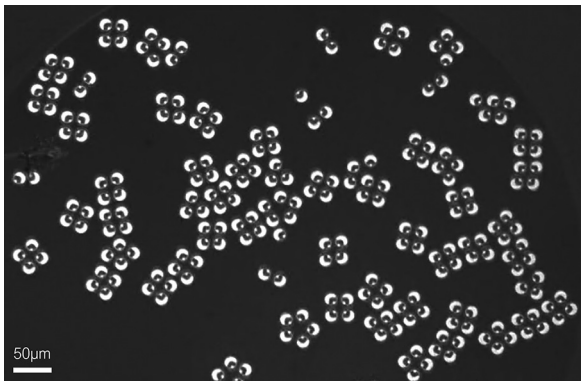

Figure 4: Optical microscope image of the product of several cycles of magnetic cyclic driving, where almost all panels have assembled into tetramers.

References:

[1] Hayakawa, Daichi, et al. Proceedings of the National Academy of Sciences 119.43 (2022): e2207902119.

[2] Long, Cheng, and Jonathan V. Selinger. Soft Matter 19.3 (2023): 519-529.

[3] Berengut, Jonathan F., et al. ACS nano 14.12 (2020): 17428-17441.

[4] Cui, J., Huang, TY., Luo, Z. et al. Nature 575, 164-168 (2019).

[5] Du, Chrisy Xiyu, et al. Soft Matter 18.34 (2022): 6404-6410.

[6] Niu, Ran, et al. Proceedings of the National Academy of Sciences 116.49 (2019): 24402-24407.